RSC Applied Polymers

ROYAL SOCIETY OF CHEMISTRY

PAPER

View Article Online
View Journal | View Issue

Open Access Article. Published on 02 spalio 2024. Downloaded on 2025-08-07 08:12:29.
This article is licensed under a Creative Commons Attribution 3.0 Unported Licence.

Check for updates

Cite this: *RSC Appl. Polym.*, 2024, **2**, 1157

Valorization of shoe sole waste into high-performance cationic dye sorbents *via* sulfonation†

Mark Robertson, Andrew Barbour and Zhe Qiang *

Ethylene-vinyl acetate (EVA)-based copolymers are widely employed in various applications such as packaging, adhesives, and shoe soles due to their relatively low cost and versatile properties, which are controlled by their chemical composition. Noteworthily, EVA in shoe soles is commonly crosslinked, which is necessary to increase their melt strength and other material properties for durable use. However, this crosslinked nature precludes traditional melt reprocessing to address the end-of-life of crosslinked EVA materials, posing a critical sustainability challenge for waste management which necessitates new recycling methods. This work develops a simple sulfonation-based method to valorize virgin EVA and shoe soles from real-world waste, imparting sulfonic acid groups on to the polymer backbones, while partially retaining the macroscopic foam structures. The reaction kinetics of sulfonation-based functionalization and their impact on the development of pore structures of EVA and their derived shoe wastes are systematically investigated. Importantly, the presence of acid groups from the upcycled shoe wastes leads to strong interactions with cationic micropollutants, enabling their high performance as sorbent materials for water remediation. The resulting materials can efficiently remove methylene blue and crystal violet from aqueous solution, exhibiting high sorption capacity and fast kinetics. Collectively, this work demonstrates a simple method to convert real-world shoe sole waste into value-enhanced sorbent products with high potential to address emerging micropollutant threats.

Received 14th September 2024,
Accepted 1st October 2024

DOI: 10.1039/d4lp00281d

rsc.li/rscapplpolym

1. Introduction

Copolymers composed of ethylene and polar repeating units represent an important class of high value commodity materials, whose properties can be tuned by their chemical composition for addressing various applications, such as adhesives, packaging films, and foams. In these systems, ethylene monomers are typically polymerized with the presence of a variety of different polar vinyl comonomers, including vinyl esters, vinyl acrylates, and acrylic acids under reaction conditions similar to established methods for low-density polyethylene (LDPE) synthesis. Generally, radical polymerization greatly favors the insertion of polar monomers like vinyl esters, acrylates, and acrylic acids, resulting in their relatively low incorporation into polyolefin backbones (<20 wt% of the comonomers). However, ethylene and vinyl acetate monomers exhibit very similar reactivity in free radical polymerization,[1] and this feature enables the synthesis of ethylene-vinyl acetate (EVA) copolymers with access to a wide range of vinyl acetate contents (from 0%–100%),[2] controlled by adjusting the relative molar ratio of these two monomers. As a result, the varied chemical composition of EVA-based polymers leads to the control over their material properties, including crystallinity, glass transition temperatures, and solubility; here we note that EVA copolymers make up the majority of all polyethylene copolymer production which is estimated to be 4.8 million tons in 2024.[3,4]

The broad use of EVA in consumer products requires the development of effective recycling methods to sustainably manage their end-of-life, preventing them from becoming landfilled or incinerated, which can lead to the formation of microplastic pollutants and greenhouse gas. To "close-the-loop" of plastic materials, mechanical recycling is a widely employed method. However, it can result in downgraded material properties and processability of the recovered products due to the process involving high temperature and high shear environments. To reduce the negative impacts of re-

School of Polymer Science and Engineering, The University of Southern Mississippi, Hattiesburg, MS, USA 39406. E-mail: zhe.qiang@usm.edu

† Electronic supplementary information (ESI) available: Gel fraction, differential scanning calorimetry, thermogravimetric analysis results in air, additional scanning electron microscopy images, and fitting results from adsorption experiments. See DOI: https://doi.org/10.1039/d4lp00281d

© 2024 The Author(s). Published by the Royal Society of Chemistry

Open Access Article. Published on 02 spalio 2024. Downloaded on 2025-08-07 08:12:29.
This article is licensed under a Creative Commons Attribution 3.0 Unported Licence.

cycling on EVA material properties, multiple studies have investigated alternative recycling methodologies, such as the conversion of EVA into dynamically crosslinked networks with improved mechanical performance retention upon multiple reprocessing cycles.[5–7] While these methods represent an effective strategy for increasing the properties of recycled EVA materials with potentially enhanced product value, they often involve multiple processing steps, and cannot be applied to address crosslinked EVA wastes. In fact, greater than 50% of EVA produced is employed to manufacture crosslinked foams, which are primarily utilized in the soles of shoes within the footwear industry. Therefore, developing methods to repurpose and enhance the value of crosslinked EVA waste is crucial for advancing environmental sustainability.

Currently, conventional methods for recycling crosslinked EVA copolymer-based post-consumer wastes primarily rely on mechanical grinding, which converts the foams to usable powders with small particle sizes. The deconstructed foams can then be employed as fillers in various composites including virgin polymer/waste EVA blends for flexible foam production and polymer-toughened cements.[8–12] For instance, Li *et al.* demonstrated that deconstructing waste EVA from the footwear industry through solid-state shear milling enabled the production of micron-sized porous particles, which could then be blended with thermoplastic polyurethane and subsequently foamed *via* supercritical carbon dioxide to generate new composite materials.[8] Using this method, the composite foam containing recycled EVA exhibited reduced residual strains after compression, as well as enhanced compressive strengths, indicating that these waste-containing products could be re-used in the original intended use in footwear. While these methods for recycling crosslinked EVA are effective for waste repurposing, they can involve multiple processing steps and potentially limit the value of the starting material.

Alternatively, upcycling of crosslinked EVA wastes could be accomplished by employing chemical functionalization to enhance their performance. For instance, Leibfarth *et al.* have developed a versatile platform for functionalizing hydrocarbon chains that can be employed to upcycle polyolefin-derived consumer products through the addition of different functional groups, including various ionic functionalities.[13] It is noteworthy that ionic functionalization of commodity polymers can also be employed to tune their chemical properties, which can be leveraged to increase their affinity toward guest molecules such as environmental contaminants. Currently, industrial and agricultural activities have resulted in the increased contamination of water sources with multitudes of different organic and inorganic micropollutants. The presence of inorganic metal cations like mercury, lead, and cadmium, among others, and organic cations from the textile and agriculture industries has been linked to multiple negative health effects in exposed populations.[14,15] Functionalizing polymer materials with anionic functionalities has previously been leveraged to remediate these cationic pollutants from contaminated water.[16] In particular, many commercial ion-exchange resins derived from highly crosslinked styrene/divinyl benzene copolymers containing acidic functional groups can be used to remove specific pollutants from aqueous media.[17] As an example, Dawson *et al.* synthesized hypercrosslinked polymers from styrene and divinyl benzene monomers which were functionalized with sulfonic acid functional groups for the targeted adsorption of heavy metal ions.[18] The polymers exhibited high adsorption capacities for cesium and strontium even in the presence of other competing cations like sodium and potassium. Liu *et al.* employed a sulfonated polystyrene-based resin system for the removal of a cationic micropollutant, specifically methylene blue, from water with high efficiencies.[19] While these materials have demonstrated excellent capacities for removing cationic contaminants, their widespread use in the water treatment industry can be prohibited by production costs and challenges in sourcing raw materials. Currently, the functionalization of EVA copolymers for the purpose of water remediation has not been thoroughly explored in the literature. Some works have employed sulfonation of EVA for improved adhesive properties, but only employ the functionalization as a surface treatment, limiting the utility of the resulting materials.[20] Previous works have demonstrated that poly(ethylene-*co*-vinyl alcohol) (EVOH) copolymers, the hydrolyzed counterpart of EVA copolymers, can be functionalized through reacting various sulfonating reagents like sulfosuccinic acid and chlorosulfonic acid with the free hydroxyls attached to the repeat unit to improve the material's ability to adsorb ions for applications as actuators and materials for blood clot prevention.[21,22] However, these functionalization processes could be challenging to apply to EVA waste materials as they require multiple reaction steps to achieve the final products. Developing simple methods to upcycle waste materials into sulfonated resins could enable their widespread use across many applications.

This work demonstrates a simple approach for the conversion of crosslinked EVA copolymer wastes, sourced from discarded shoe soles (real-world waste), into sulfonic acid-functionalized sorbents for the remediation of chemical contaminants from aqueous media. Importantly, the versatility of the upcycling strategy developed herein enables the upcycling of waste with unknown compositions, which can be exceedingly challenging, yet vital for addressing plastic waste management in practice. Specifically, our approach involves a one-step treatment to functionalize the EVA-derived materials, resulting in a high content of sulfonic acid moieties along the polymer backbone. During this process, portions of the inherent cell structures of the crosslinked and foamed waste materials can be retained. We note that previous works using similar techniques to sulfonate polyolefins require long reaction times due to diffusion limitations, but the presence of the vinyl acetate repeat unit and fuming sulfuric acid as the sulfonating agent accelerates the functionalization process. Using this method, shoe sole waste can become high performance sorbents for removing cationic contaminants from aqueous media, with high sorption capacity and fast kinetics. This work demonstrates an efficient route for repurposing crosslinked EVA

 © 2024 The Author(s). Published by the Royal Society of Chemistry

Open Access Article. Published on 02 spalio 2024. Downloaded on 2025-08-07 08:12:29.
This article is licensed under a Creative Commons Attribution 3.0 Unported Licence.

waste, typically found in the footwear industry, into highly functional materials for environmental remediation.

2. Experimental section

2.1 Materials

Ethylene-vinyl acetate (EVA) (M_n = 150 000 g mol^{-1}, vinyl acetate content = 40 wt%) was obtained from Scientific Polymer Products Inc., which was used as a model system, and the crosslinked EVA foams were sourced from used footwear from two different brands. Fuming sulfuric acid (20%–30% free SO_3) was purchased from Fisher Scientific and methylene blue hydrate and crystal violet hydrate were purchased from TCI Chemicals. Sodium chloride (NaCl, 99.0%) was purchased from VWR, and sodium hydroxide (NaOH, >98%) and phenolphthalein were purchased from Sigma-Aldrich. All compounds were used as received. Deionized water was produced through filtering tap water with a Millipore Mill-Q Type 1 filtration system.

2.2 Preparation of sulfonic acid-functionalized polymers

The shoe soles were cut into 10 mm × 10 mm × 10 mm cubes prior to reaction. In a typical sulfonation reaction, 500 mg of the EVA polymer or crosslinked waste foams were introduced into a 100 mL reaction vessel and 25 mL of fuming sulfuric acid was added to the vessel. It is worth noting that the reaction mixture was not stirred, and the individual shoe waste cubes were weighted down with glass Pasteur pipettes to ensure they remained submerged in the acid. The vessel was then placed into a crystallization dish filled with thermal beads (Lab Armor) heated using a hotplate at 150 °C. After the desired reaction time, the vessel was removed from the crystallization dish and allowed to cool, and the contents were separated using a glass fritted funnel. After the acid was removed, the polymer was thoroughly washed with deionized water (200 mL at least 3 times) to remove residual acid and byproducts. After washing, the polymer was dried under vacuum at 60 °C for 4 h before use.

2.3 Characterization

A Nicolet 6700 spectrometer (Thermo Fisher) with an attenuated total reflectance (ATR) attachment was employed for Fourier transform infrared (FTIR) spectroscopy experiments using 32 scans with a resolution of 1 cm^{-1}. Gel fraction studies were performed by submerging the samples in dichloromethane (DCM) for 24 h and measuring the remaining mass after drying under vacuum at 30 °C for 3 h. Thermogravimetric analyses were performed on a Discovery 550 thermogravimetric analyzer (TGA) from TA Instruments. The samples were heated from room temperature to 800 °C at a ramp rate of 10 °C min^{-1} under a nitrogen atmosphere. TGA experiments were also performed in air to determine the residual inorganic contents of the foams by heating the samples to 800 °C with a ramp rate of 10 °C min^{-1}. Differential scanning calorimetry (DSC) experiments were conducted using a Discovery 250 DSC from TA Instruments. A heat–cool–heat procedure was used from −90 °C to 200 °C at a ramp rate of 10 °C min^{-1} during heating and 5 °C min^{-1} during cooling. The amount of acid incorporated through the sulfonation procedure was determined through Mohr's titrations, following an established method. Briefly, the sulfonated samples were soaked in 0.25 M NaCl for 24 h to exchange the protons of the sulfonic acid with sodium ions. The resulting solution was titrated with 0.025 M sodium hydroxide solution using phenolphthalein as an indicator. The amount of sulfonic acid installed in the polymer was determined using the following equation:

$$\text{Acid content} = \frac{V_{\text{NaOH}} M_{\text{NaOH}}}{m_{\text{p}}}, \quad (1)$$

where V_{NaOH} is the volume of NaOH used to achieve pH 7 (L), M_{NaOH} is the molarity of the NaOH solution (mmol L^{-1}), and m_{p} is the mass of the polymer sample (g). Scanning electron microscopy (SEM) images were recorded using a Zeiss Ultra 60 field-emission scanning electron microscope with an accelerating voltage of 17 kV. Nitrogen physisorption experiments were carried out at 77 K to investigate the sulfonated polymer porosity. The Brunauer–Emmett–Teller (BET) method was employed to determine the specific surface area. Ultraviolet-visible (UV-vis) spectroscopy experiments were conducted with a Genesys 30 visible spectrophotometer from Thermo Scientific using a wavelength range of 400–700 nm at a resolution of 1 nm using a quartz cuvette as the sample holder.

2.4 Adsorption experiments

Adsorption experiments were conducted using methylene blue hydrate and crystal violet hydrate as model cationic micropollutants. Solutions of each dye were prepared at known concentrations (in the range of 1–15 mg mL^{-1}) and measured through UV-vis spectroscopy to determine the extinction coefficients of the dye molecules using the Beer–Lambert law (eqn (2)):

$$A = \varepsilon b C, \quad (2)$$

where A is the absorbance measured through UV-vis, ε is the extinction coefficient, b is the path length, and C is the concentration of the solution. The extinction coefficients were then employed to determine the concentration of dye in the solution after adsorption, and thus used to calculate the amount of dye adsorbed by the sorbent. All adsorption experiments were carried out at a sorbent dosage of 0.4 mg mL^{-1} and all sorbents were dried under high vacuum at 60 °C for 12 h prior to the adsorption experiment. To study the adsorption kinetics of both dyes, the sorbents were added to 50 mg L^{-1} dye solutions and shaken at 800 rpm using a Basic Vortex Mixer from Thermo Scientific. At regular time intervals, 50 μL were removed and diluted to 1 mL with DI water for UV-vis measurements. The quantity of dye adsorbed was calculated using eqn (3):

$$q = \frac{(C_0 - C_t)V}{M}, \quad (3)$$

Open Access Article. Published on 02 spalio 2024. Downloaded on 2025-08-07 08:12:29.
This article is licensed under a Creative Commons Attribution 3.0 Unported Licence.

where q is the quantity adsorbed (mg g^{-1}), C_0 is the initial concentration (mg L^{-1}), C_t (mg L^{-1}) is the concentration of dye after a given time, V is the volume of the dye solution (L), and M is the mass of the sorbent used in the adsorption experiment (g). The adsorption kinetics results were fit to a pseudo-second order model using eqn (4):

$$\frac{t}{Q_t} = \frac{t}{Q_e} + \frac{1}{kQ_e{}^2}, \tag{4}$$

where Q_e is the quantity of dye adsorbed at equilibrium, Q_t is the quantity of dye adsorbed at a given time, t, and k is the rate constant. Adsorption isotherms were developed using the same procedure (0.4 mg mL^{-1} sorbent dosage, 800 rpm) in dye solutions ranging in concentration from 50 mg L^{-1} to 400 mg L^{-1}. After 12 h of adsorption, aliquots were taken for UV-vis measurements. The resulting isotherms were fit to both Langmuir and Freundlich models using eqn (5) and (6), respectively:

$$Q_e = \frac{C_e}{\frac{1}{kQ_m} + \frac{C_e}{Q_m}}, \tag{5}$$

where Q_e is the quantity of dye adsorbed at equilibrium, C_e is the concentration of dye at equilibrium, k is the adsorption capacity constant, and Q_m is the maximum adsorption capacity.

$$Q_e = kC_e^{1/n}, \tag{6}$$

where Q_e is the quantity of dye adsorbed at equilibrium, C_e is the concentration of dye at equilibrium, k is the adsorption capacity constant, and n is a constant that describes the heterogeneity of adsorption sites.

3. Results and discussion

3.1 Midsole waste characterization

Shoe midsoles represent a common class of EVA copolymer-derived materials that are challenging to repurpose or recycle into new products at the end of their intended service life. This difficulty is associated with their crosslinked nature, which is necessary to provide the polymer with sufficient melt strength and to enhance their performance durability.[23] However, their crosslinked nature prevents the melt processing of EVA waste materials into new products. As a result, innovative recycling methods and alternative end-of-life solutions must be developed to address the sustainability challenges posed by these materials. This work demonstrates an effective method for producing functional sorbent materials for water remediation from crosslinked EVA wastes through a solid-state reaction that installs sulfonic acid functionalities into the polymer matrix. In turn, the additional functionality can be employed to tune interactions between the polymer material and cationic micropollutants, as demonstrated in Fig. 1. In particular, this work focuses on foams from two different brands of athletic shoes (discarded after being used for ~5 years by the first author) that are used as model waste precursors, referred to as Brand 1 and Brand 2, respectively. Gel fraction experiments in dichloromethane indicate gel fractions of 97% and 96% for Brand 1 and Brand 2, respectively, while a commercially available virgin EVA copolymer can be completely dissolved, confirming that the waste foams are crosslinked from production (Fig. S1†). We note that, typically, EVA copolymers are crosslinked through a peroxide-initiated reaction which primarily occurs at the ester of the vinyl acetate repeat units.[5]

The chemical compositions of the shoe soles and the virgin EVA copolymer were first investigated through Fourier transform infrared (FTIR) spectroscopy experiments which are displayed in Fig. 2(A). The virgin EVA copolymer and the two waste foam samples exhibit alkyl stretching vibrations between 3000 cm^{-1} and 2800 cm^{-1}, which are a result of the olefinic backbone of the copolymer. Additionally, all three samples exhibit characteristic bands associated with the vinyl acetate repeat units. Specifically, the bands at 1740 cm^{-1}, 1237 cm^{-1}, and 1020 cm^{-1} are assigned to the C=O, C–C–O, and C–O bonds of the vinyl acetate repeat units, respectively. It is worth noting that there are multiple dissimilar bands in the spectra of the shoe soles compared to the virgin EVA system, which is likely a result of additives included for processing and performance enhancement. We note that the crosslinked nature of the shoe foams makes quantifying the amount of vinyl acetate incorporation through solution state spectroscopic techniques such as nuclear magnetic resonance spectroscopy

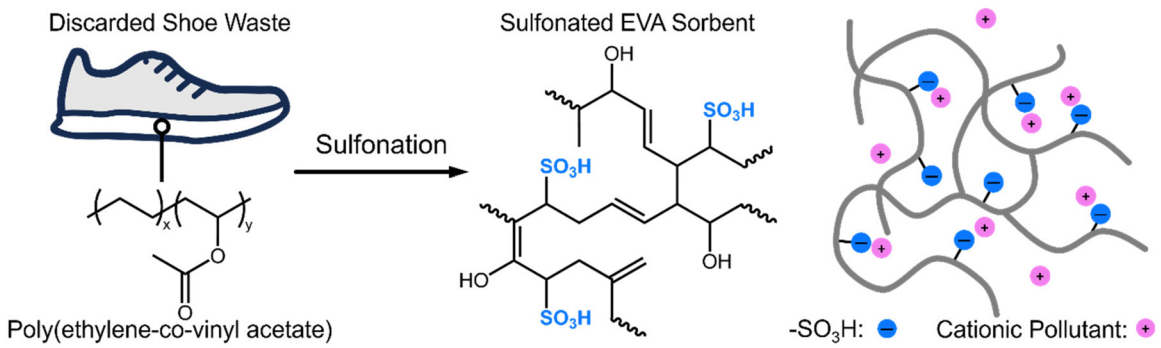

Fig. 1 Schematic illustration of employing discarded shoe waste midsoles as precursors for producing sulfonated polymer sorbents to address micropollutant contamination.

 © 2024 The Author(s). Published by the Royal Society of Chemistry

Open Access Article. Published on 02 spalio 2024. Downloaded on 2025-08-07 08:12:29.
This article is licensed under a Creative Commons Attribution 3.0 Unported Licence.

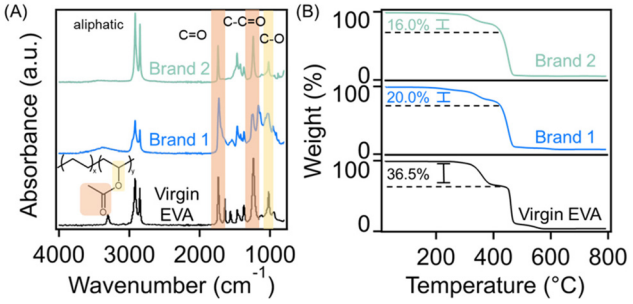

Fig. 2 (A) FTIR spectra and (B) TGA thermograms of the EVA copolymer and waste shoe soles. The FTIR and TGA results are vertically shifted for clarity.

challenging. However, the TGA thermograms in Fig. 2(B), which were recorded under a nitrogen atmosphere, depict 2 distinct degradation steps which are associated with vinyl acetate and ethylene repeat unit degradation; this result can be leveraged to estimate their relative amounts. The virgin polymer exhibits a degradation onset at 327 °C which results in a 36.5% mass decrease, followed by a secondary degradation starting at 452 °C. The degradation at lower temperatures typically corresponds to the decomposition of vinyl acetate repeat units and is in good agreement with previously determined literature values.[24] Therefore, this suggests that the EVA copolymer is composed of 36.5% vinyl acetate repeat units by mass (manufacturer's specification is 40% by mass). We note consistency of the mass loss at lower temperatures of the uncrosslinked virgin EVA and the manufacturer's specification indicates the accuracy of using TGA results to estimate vinyl acetate content. In this study, Brand 1 and Brand 2 exhibit onsets of degradation at similar temperatures of 294 °C and 302 °C, respectively, with mass losses that indicate the presence of 20.0 wt% and 16.0 wt% vinyl acetate repeat units within the polymer foams. These results are further supported in the DSC thermograms in Fig. S2† as well as in additional discussion which can be found in the ESI.†[24,25] Additionally, the residual masses depicted in the TGA thermograms of Brand 1 and Brand 2 are 7.0 wt% and 6.5 wt%, respectively, which can be associated with the presence of inorganic fillers that are commonly included to alter the polymer optical or mechanical properties, as confirmed through additional TGA experiments conducted in air, as presented in Fig. S3.†

3.2 Functionalization through sulfonation-induced crosslinking

The EVA copolymer-derived materials were functionalized through a solid-state sulfonation reaction, which has been established in the literature for converting polyolefins into sulfonated crosslinked polymers for various applications.[25–27] At elevated temperatures with the presence of a sulfonating agent like concentrated sulfuric acid, fuming sulfuric acid, or chlorosulfonic acid, sulfonic acid groups can be introduced into the olefinic polymer backbone, which can also dissociate to form alkenes that lead to radical initiation and thus enables the formation of intermolecularly crosslinked polymer chains.[28–30]

The progress of this reaction can be monitored as a function of time through multiple characteristic bands in the FTIR spectra depicted in Fig. 3(A–C). It is important to note that the characteristic bands of the EVA-derived precursor change as a function of the sulfonation reaction, making it very challenging to normalize spectra to any internal standard. Therefore, only qualitative conclusions regarding the presence of functional groups can be made through analysis of these results. Specifically, the contributions from the alkyl stretching vibrations between 3000 cm^{-1} and 2800 cm^{-1} are no longer present after 5 min of reaction across all three samples upon the addition of sulfonic acid groups. The presence of sulfonic acid functionalities is indicated by the bands at 1107 cm^{-1} and 1010 cm^{-1} which correspond to the symmetric and asymmetric stretch, respectively, of the sulfonic acid. Generally, these bands are present at all reaction times for all three samples, indicating that the addition of sulfonic acid groups occurs very readily. Additionally, the weak stretch at 1665 cm^{-1} and the vibration at 875 cm^{-1} observed in all samples are associated with the introduction of alkenes, due to dissociation of some of the sulfonic acid groups from the polymer backbones during the crosslinking process. It is also worth noting that even at short reaction times, the previously identified bands that are associated with the vinyl acetate repeat unit are no longer present in the spectra. This could suggest that the highly acidic conditions drive the hydrolysis of the ester within the repeat unit, resulting in the conversion of the ester into hydroxyl functionalities, which has been observed in the literature.[31]

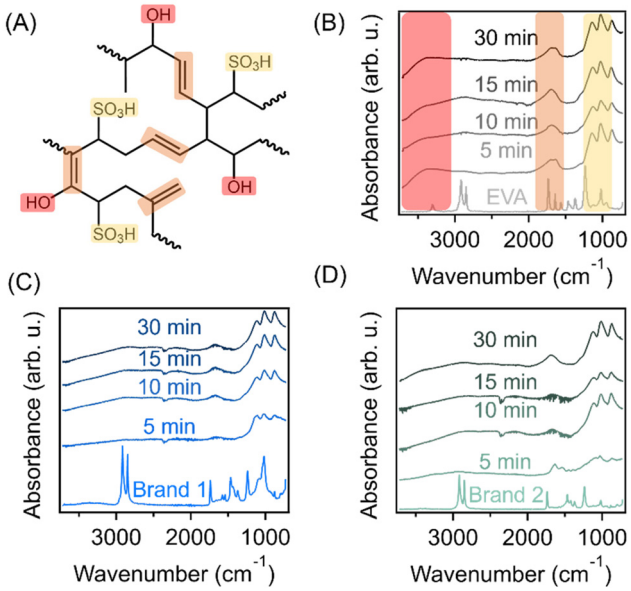

Fig. 3 (A) Generalized chemical structure of crosslinked EVA through the sulfonation-induced crosslinking process with the characteristic functional groups highlighted to correspond with the highlighted regions in the FTIR spectrum. FTIR spectra of (B) the virgin EVA precursor, (C) Brand 1, and (D) Brand 2 as a function of sulfonation time.

Open Access Article. Published on 02 spalio 2024. Downloaded on 2025-08-07 08:12:29.
This article is licensed under a Creative Commons Attribution 3.0 Unported Licence.

In addition to FTIR spectroscopy results, the progress of the sulfonation-induced crosslinking process can be monitored through determining the amount of acid incorporated into the polymer *via* Mohr's titrations; these results are provided in Fig. 4. After very short reaction times (5 min), the acid content is essentially saturated in the virgin EVA copolymer sample. The acid content value after 5 min of reaction is 7.1 mmol g^{-1}, which slightly varied throughout the progress of the reaction. We found that the incorporation of acid into both waste foams exhibits slower kinetics compared to the virgin EVA material. This is an interesting observation, as the sulfonation temperature for reacting the EVA components of these waste materials (150 °C) was above both the melting point and the glass transition temperature (T_g, typically between −50 °C and 0 °C) of the polymer. The sulfonating agent should readily diffuse throughout the material and allow for the reaction to occur. However, despite the porous nature of the post-consumer waste foams which should facilitate the transport of the sulfuric acid into the polymer system, the sulfonation kinetics are slower than that in the virgin polymer. One explanation could be associated with the increased vinyl acetate content in the virgin EVA material which can be hydrolyzed through acid-catalyzed hydrolysis, thus increasing the hydrophilicity of the material to facilitate the sulfonation reaction; the enhanced hydrophilicity at short reaction times may allow for the diffusion to occur throughout the solid polymer more readily. While the kinetics are slightly reduced, the maximum acid content is achieved after only approximately 30 min of reaction, reaching values of 11.4 mmol g^{-1} and 13.6 mmol g^{-1} for Brand 1 and Brand 2, respectively. It is worth noting that the reaction kinetics for the sulfonation of the EVA-derived materials is greatly enhanced compared to those of other polyolefin materials that have been reported before. For instance, thermoplastic elastomers containing a saturated polyolefin backbone, such as poly(styrene)-*block*-poly(ethylene-*ran*-butylene)-*block*-poly(styrene), as well as semicrystalline polypropylene and PE can require multiple hours of sulfonation using concentrated sulfuric acid to achieve similar results.[32,33] There are multiple reasons for the enhanced reaction kinetics in the EVA system presented here. Firstly, fuming sulfuric acid is employed as the sulfonating agent which is known to be more highly reactive than concentrated sulfuric acid due to the increased presence of free SO_3 moieties. Secondly, as the sulfonation reaction of polyolefin materials is typically diffusion-controlled, the incorporation of the vinyl acetate repeat unit into polymer backbones improves their hydrophilicity, thus facilitating the sulfonating agent to penetrate and react more readily. Moreover, after the sulfonation reaction, the waste foams exhibit higher acid contents in comparison with the EVA copolymer as well as other commercial sulfonated polymer resins. For comparison, Amberlyst-15™, a commercial ion exchange resin with sulfonic acid functionalities derived from hyper-crosslinked styrenic polymers, has an acid content of 4.66 mmol g^{-1}. Similarly, multiple literature examples which employ sulfonic acid-functionalized, hyper-crosslinked materials typically exhibit acid loadings between 3 mmol g^{-1} and 5 mmol g^{-1};[34,35] these values are all lower in comparison with both the crosslinked EVA and the waste-derived sorbents presented here. This is likely a result of these styrenic hyper-crosslinked polymers being limited to the addition of 1 sulfonic acid per styrene repeat unit while having a much higher repeat unit molecular weight than that of the EVA copolymer. When normalized by the mass of the sulfonated polymer, the EVA-derived materials have higher acid contents, while the number of functionalized repeat units may be similar. Previously, Woodward *et al.* demonstrated a one-pot approach for synthesizing sulfonated hyper-crosslinked polymers using 4,4′-bis(chloromethyl)biphenyl as a monomer and chlorosulfonic acid as a catalyst for polymerization and a sulfonating agent,[36] which resulted in a sulfonic acid content of 3.76 mmol g^{-1}, with demonstrated utility as solid acid catalysts for the acid-catalyzed hydrolysis of cyclohexyl acetate to cyclohexanol. This result indicates the heightened potential of these waste-derived materials for multiple applications.

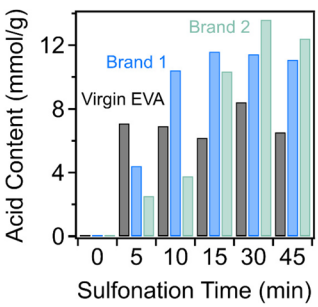

Fig. 4 Amount of acid incorporated into virgin EVA, Brand 1, and Brand 2 as a function of reaction time determined through titrations.

The sulfonation reaction may impact the macroscopic structures of the polymer precursors, which was investigated through scanning electron microscopy (SEM) images as presented in Fig. S4.† The virgin EVA material was smooth pellets (Fig. S4(A)†) and became significantly distorted at short reaction times (Fig. S4(B and C)).† The surface of the polymer particle becomes highly cracked, which has been previously elucidated as a mechanism for assisting diffusion of the sulfuric acid throughout the solid material.[33] This cracked macroscopic structure is retained throughout the 30 min reaction process (Fig. 5(A)). The post-consumer foams exhibit different structural changes during the sulfonation reaction. At short times (Fig. S4(E and H)†), only the outer surface of the foams is reacted, while the closed-cell foam structure is retained in the interior of the sample. However, after 15 min of reaction (Fig. S4(F and I)),† both foams exhibit partial deterioration of the original macroporous structures, which were then retained throughout the remainder of the reaction up to 30 min. Specifically, from these SEM images in Fig. 5(B and C), it is determined that the foam structure can partially deteriorate into thin platelets that once made up the walls of the closed-cell structures. The pore textures of the sulfonated materials were further investigated through nitrogen physisorption experiments, and their liquid nitrogen sorption isotherms are

 © 2024 The Author(s). Published by the Royal Society of Chemistry

Open Access Article. Published on 02 spalio 2024. Downloaded on 2025-08-07 08:12:29.
This article is licensed under a Creative Commons Attribution 3.0 Unported Licence.

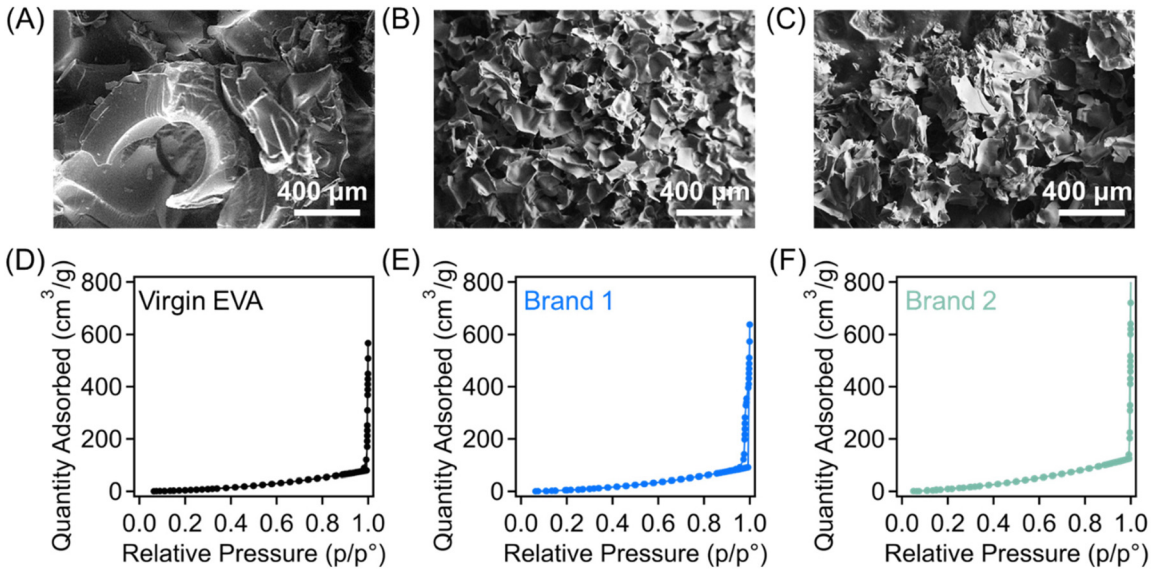

Fig. 5 SEM micrographs of sulfonated (A) EVA, (B) Brand 1, and (C) Brand 2 foams after 30 min of reaction. Nitrogen physisorption isotherms of the corresponding sample, including sulfonated (D) EVA, (E) Brand 1, and (F) Brand 2 foams.

presented in Fig. 5(D–F). All three samples exhibit Type III isotherms with no hysteresis, indicating the absence of micropores and mesopores. The sharp increase in the quantity of nitrogen adsorbed at high relative pressures is indicative of the presence of macropores, which is consistent with the foam nature of their precursor materials. From these results, it was found that despite the retention of macropores, the sulfonated materials from EVA and shoe wastes generally exhibit very low BET specific surface areas (<10 m^2 g^{-1}), indicating that the functionalization reaction does not lead to the formation of micropores.

3.3 Employing shoe midsole waste derived sorbents for water remediation

Adsorption is a widely used method for removing chemical contaminants from wastewater due to the ease-of-use and low operation cost. Sulfonic acid functional groups have been commonly leveraged for the remediation of various micropollutants including antibiotics and organic dye molecules.[37,38] The strongly acidic nature of sulfonic acid functional groups enables them to be deprotonated very easily, which can provide an abundance of negatively charged sites within polymeric sorbents that have favorable electrostatic interactions with cationic pollutants. In this work, adsorption performances of sulfonated EVA-derived sorbents were studied with two model cationic organic dyes, including methylene blue hydrate (Fig. 6(A)) and crystal violet hydrate (Fig. 6(D)). Methylene blue and crystal violet are both dyes that are widely employed in the textile industry, among many other applications, which have been found to be toxic and carcinogenic and are a source of contamination in many water sources.[39,40] Additionally, these two molecules vary in molecular size and geometry, allowing the investigation of size effects on the removal of the contaminants from water using our upcycled polymers. These molecules could also act as analogs to other cationic contaminants, such as paraquat and diquat, that are prevalent contaminants used as herbicides in the agricultural industry.[41] Systematic experiments were performed to illustrate the efficacy of the sulfonated materials for the removal of cationic micropollutants, including their sorption mechanisms and kinetics. Specifically, adsorption experiments were performed at a sorbent dosage of 0.4 mg sorbent per mL of dye solution and a concentration of 50 mg L^{-1}. Aliquots were taken at regular time intervals and ultraviolet-visible (UV-vis) spectroscopy was employed to determine the changes in concentration as adsorption occurred.

As demonstrated in Fig. 6(B and E), the intensity of the absorption peak of dye-polluted water solution decreases with increasing time during the adsorption experiment which corresponds to a decrease in the concentration of the cationic dye as it is adsorbed by the polymer sorbent. At a solution concentration of 50 mg L^{-1} and a sorbent dosage of 0.4 mg mL^{-1}, the sulfonated sorbent derived from virgin EVA exhibits an adsorption capacity of 85.3 mg g^{-1} after 60 min of the adsorption experiment. The sulfonated sorbents derived from the post-consumer waste materials, Brand 1 and Brand 2, have adsorption capacities of 103.3 mg g^{-1} and 97.9 mg g^{-1}, respectively. The increased adsorption capacity compared to the virgin EVA derived materials can be attributed to the increased acid content installed within the foams during the sulfonation process which promotes interactions between the sorbent and the cationic dye molecule. The adsorption of crystal violet exhibits similar results; however, the adsorption capacities of all three sorbents are reduced. The virgin EVA-derived sorbent achieves an adsorption capacity of 73.4 mg g^{-1}, while Brand 1 and Brand 2 achieve adsorption capacities of 76.5 mg g^{-1} and 48.1 mg g^{-1}, respectively. The reduced capacities against the crystal violet model dye could be a result

Open Access Article. Published on 02 spalio 2024. Downloaded on 2025-08-07 08:12:29.
This article is licensed under a Creative Commons Attribution 3.0 Unported Licence.

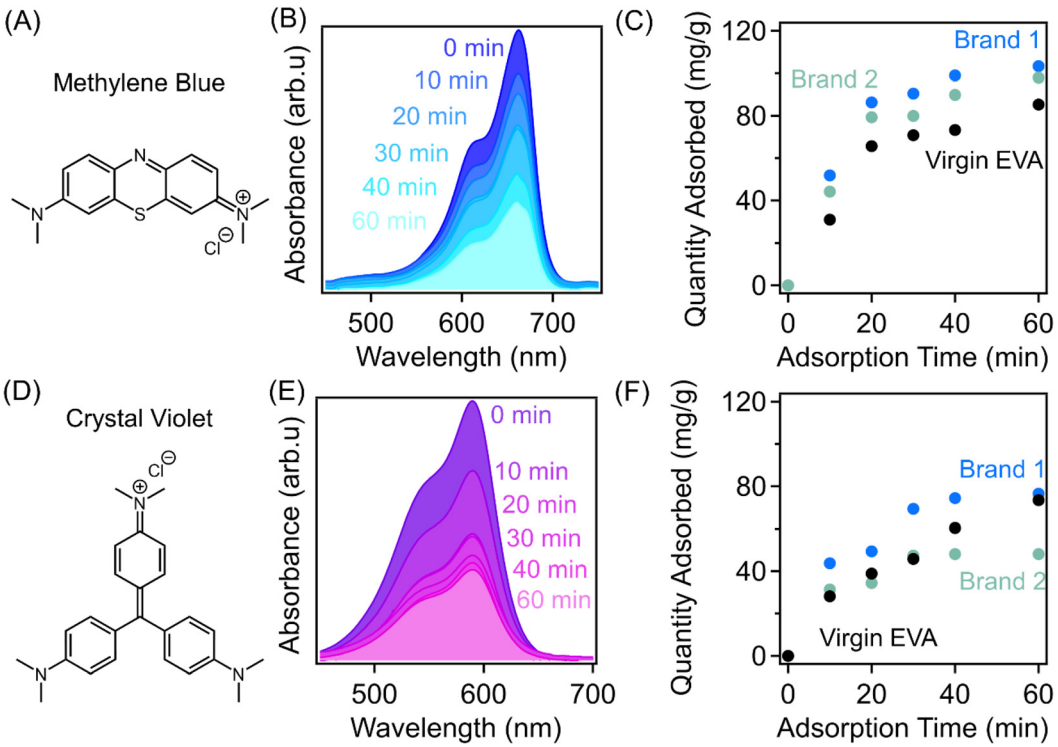

Fig. 6 (A) Chemical structure of methylene blue. (B) Representative UV-vis spectra as a function of time during the adsorption experiment. (C) Quantity of methylene blue adsorbed as a function of time by the sulfonated sorbents. (D) Chemical structure of crystal violet. (E) Representative UV-vis spectra as a function of time during the adsorption experiment. (F) Quantity of crystal violet as a function of time.

of the steric bulk of the molecule reducing its ability to diffuse throughout the sorbent in comparison with the smaller methylene blue molecule.[42] The impact of the acid content within the sorbents is further illustrated by the adsorption results of sorbents which were sulfonated for varying amounts of time, as presented in Fig. S5.† Specifically, the results for sorbents derived from virgin EVA, Brand 1, and Brand 2 post-consumer wastes sulfonated for 5 min and 15 min are compared to the sorbents sulfonated for 30 min. Generally, from these results it was found that the samples sulfonated for longer reaction times exhibit higher adsorption capacities, suggesting the impact of increasing the amount of acid functionalities on the interactions between the sorbents and the dye molecules. The effect of the reaction time is very pronounced in the post-consumer waste-derived sorbents as the acid content increases considerably with the reaction time, resulting in a greater adsorption capacity of the cationic molecules after the same contact time. For the virgin EVA-derived sorbent, the sample sulfonated for 30 min does exhibit a slightly higher adsorption capacity, which could be a result of the altered macroscopic morphology of the sorbent or additional installation of hydroxyl functionalities through hydrolysis of the acetate repeat unit.

To further investigate the impact of the crosslinked nature of the sorbents on their ability to adsorb contaminant molecules, the results have been normalized by the acid contents of the respective sorbents, which are found in Fig. S6.† Generally, the sorbents derived from precursors containing higher vinyl acetate content can adsorb more dye molecules per mmol of sulfonic acid added to the polymer precursor. These results could suggest that the precursors with greater vinyl acetate contents result in lower degrees of crosslinking due to the preferential hydrolysis of the repeat unit rather than sulfonation and subsequent crosslinking. The discrepancy in adsorption capacities is also more pronounced in the results for the adsorption of the larger molecule, crystal violet. This supports the hypothesis that the lower crosslink density can facilitate the diffusion of the molecules throughout the sorbent itself, which increases sorption site accessibility, thus resulting in higher quantities adsorbed. This result highlights the trade-off between sulfonic acid contents and crosslink density on the utility of these sorbents for water remediation.

The adsorption results were fit to a pseudo-second order kinetic model using eqn (4), and the fitting *via* using a pseudo-second order model for both methylene blue and crystal violet is shown in Fig. 7 (the fitting parameters can be found in Table S1†). Specifically, the rate constants for the virgin-EVA-, Brand 1-, and Brand 2-derived sorbents for the adsorption of methylene blue are 0.0011 g mg^{-1} min^{-1}, 0.0017 g mg^{-1} min^{-1}, and 0.0014 g mg^{-1} min^{-1}, respectively, indicating similar adsorption kinetics across all three sorbent identities. The adsorption of crystal violet exhibits rate constants of 0.0023 g mg^{-1} min^{-1}, 0.0019 g mg^{-1} min^{-1}, and 0.0060 g mg^{-1} min^{-1} for the virgin EVA-, Brand 1-, and Brand

 © 2024 The Author(s). Published by the Royal Society of Chemistry

Open Access Article. Published on 02 spalio 2024. Downloaded on 2025-08-07 08:12:29.
This article is licensed under a Creative Commons Attribution 3.0 Unported Licence.

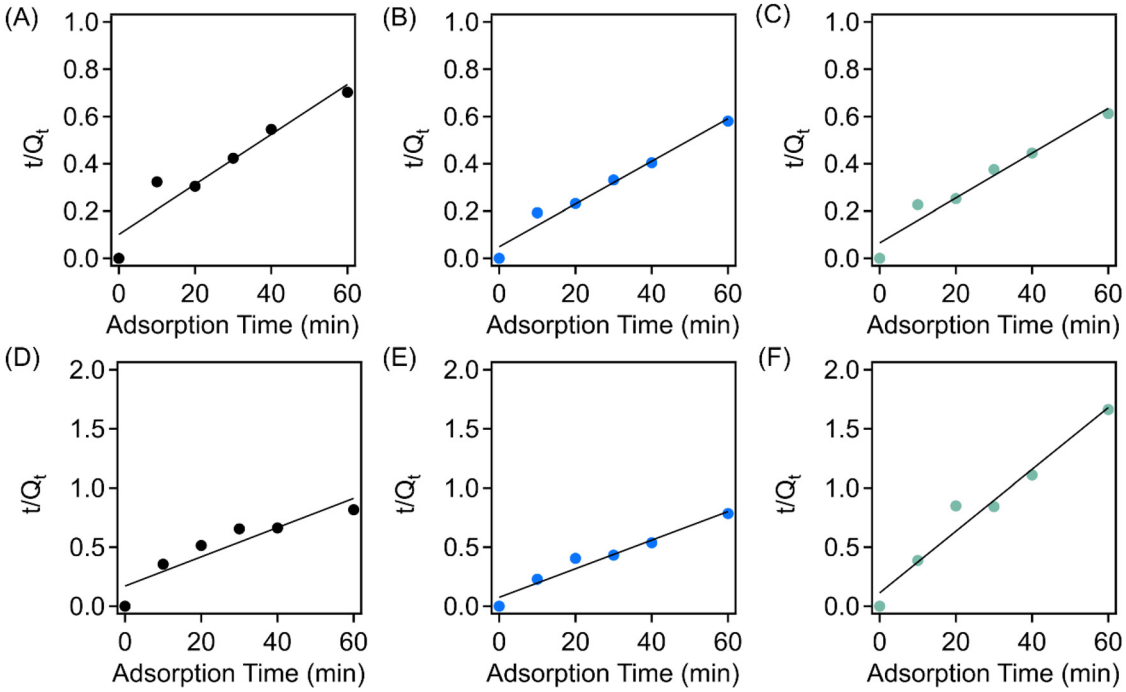

Fig. 7 Model fits to a pseudo-second order kinetic model for the adsorption of methylene blue by (A) the virgin EVA-derived sorbent, (B) Brand 1-derived sorbent, and (C) Brand 2-derived sorbent. Model fits to a pseudo-second order kinetic model for the adsorption of crystal violet by (D) the virgin EVA-derived sorbent, (E) Brand 1-derived sorbent, and (F) Brand 2-derived sorbent.

2-derived materials, respectively. These results suggest that the sorbents achieve their equilibrium adsorption capacity for taking up crystal violet more quickly than in the adsorption of methylene blue.

The adsorption kinetics and capacity of the sorbents in this work for methylene blue and crystal violet are compared to multiple different literature examples in Fig. 8(A) and (B), respectively. These results and their associated reference are also presented in Tables S2[43–58] and S3,†[59–70] respectively. From the fitting parameters for the pseudo-second order kinetic model, the EVA-derived materials exhibit some of the highest equilibrium adsorption capacities for adsorption of methylene blue from a solution concentration of 50 mg L^{-1}, although they exhibit reduced second order rate constants (k_2) when compared with several other materials in the literature. Noteworthily, most materials with larger rate constants, and thus enhanced kinetics, exhibit lower sorption capacity against methylene blue compared to the EVA-derived materials. While the results for the adsorption of crystal violet seems to be much more varied across the 3 EVA-derived materials, all three samples exhibit improved equilibrium adsorption capacity compared to reference materials with similar rate constants, indicating their high performance for taking up crystal violet dye.

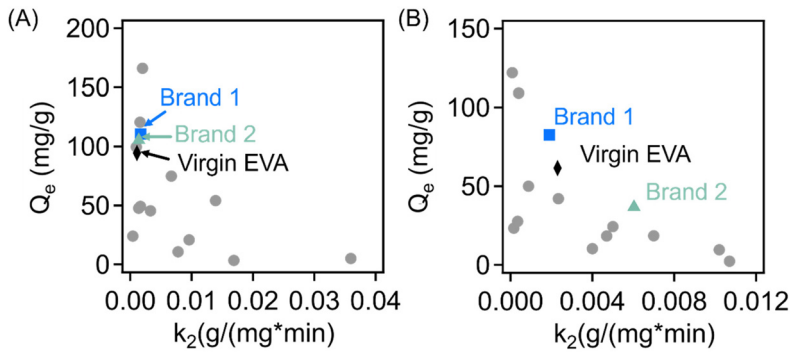

Fig. 8 Comparison of parameters from pseudo-second order fits to kinetic adsorption results for (A) methylene blue and (B) crystal violet between literature examples and the materials developed in this work; dye concentration in the solution is 50 mg L^{-1}. Brand 1: blue square; virgin EVA: black diamond; and Brand 2: green triangle.

Open Access Article. Published on 02 spalio 2024. Downloaded on 2025-08-07 08:12:29.
This article is licensed under a Creative Commons Attribution 3.0 Unported Licence.

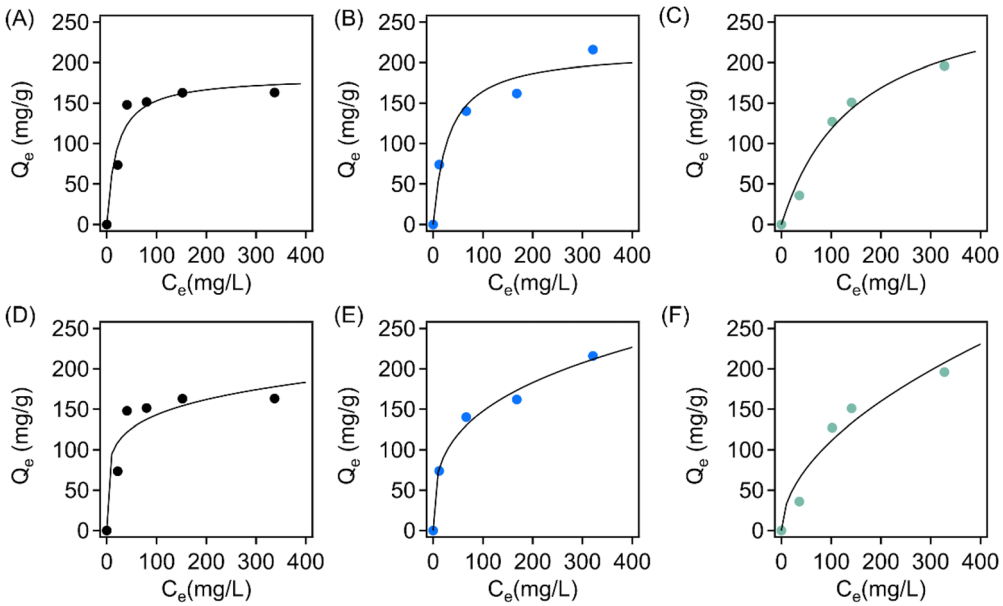

Fig. 9 Adsorption isotherms fit to a Langmuir model for the (A) virgin EVA-, (B) Brand 1-, and (C) Brand 2-derived sorbents. Adsorption isotherms fit to a Freundlich model for the (D) virgin EVA-, (E) Brand 1-, and (F) Brand 2-derived sorbents.

The adsorption mechanism and maximum equilibrium adsorption capacities for crystal violet were further investigated through characterizing their adsorption isotherms. Specifically, adsorption experiments were carried out in dye solutions with concentrations ranging from 50 mg L^{-1} to 400 mg L^{-1} using a sorbent dosage of 0.4 mg mL^{-1}. The sorbents were allowed to equilibrate over 12 h, and the quantity of dye adsorbed was then characterized through UV-vis spectroscopy. The isotherms were fit to both the Langmuir and Freundlich models using eqn (5) and (6), respectively. The resulting isotherms and their model fits are found in Fig. 9, and the fitting parameters are found in Table S2.† It is found that fits to the Langmuir model (Fig. 9(A–C)) generally have lower X^2 values, indicating a higher accuracy. From the fitting parameters, the maximum adsorption capacity for crystal violet of the virgin EVA-, Brand 1-, and Brand 2-derived sorbents are approximately 183.0 mg g^{-1}, 215.1 mg g^{-1}, and 296.9 mg g^{-1}, respectively.

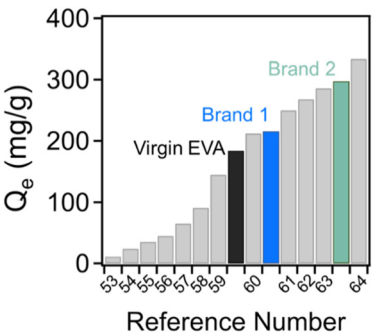

Fig. 10 Comparison of the equilibrium adsorption capacity of the shoe-waste-derived materials to the results found in ref. 53–64.

For comparison, multiple results from previous literature examples have been compiled in Fig. 10. Across many different material systems and functionalization routes, the sorbents produced through this work, including those derived from challenging-to-recycle waste materials, exhibit comparatively excellent adsorption capacities for remediating crystal violet. Although crystal violet is a model system, it could be expected that this performance could be extended to address a variety of other cationic contaminants, potentially including heavy metals and antibiotics.

4. Conclusions

Waste from the footwear industry is typically very difficult to recycle, which results in large portions being landfilled or incinerated. More specifically, the midsoles of shoes are often comprised of crosslinked EVA foams which cannot be melt-reprocessed *via* traditional mechanical recycling methods. In this work, we have developed a simple and robust method for valorizing EVA-based wastes of unknown compositions into materials that can be employed for the adsorption of environmental contaminants from water sources. Sulfonation-induced crosslinking of EVA based materials results in the installation of large amounts of sulfonic acid functional groups which are easily deprotonated, thus enhancing interactions between the sulfonated materials and cationic contaminants. The sorbents developed through this method exhibit excellent adsorption performances for two model micropollutants, methylene blue and crystal violet. This work could provide a new method for upcycling traditionally challenging-to-recycle materials that can be broadly applied for water remediation.

 © 2024 The Author(s). Published by the Royal Society of Chemistry

Open Access Article. Published on 02 spalio 2024. Downloaded on 2025-08-07 08:12:29.
This article is licensed under a Creative Commons Attribution 3.0 Unported Licence.

Author contributions

This work was conceptualized by M. R. and Z. Q., who also designed all experiments. M. R. and A. B. carried out material preparation and all experiments, which were overseen by Z. Q. All authors contributed to writing the manuscript.

Data availability

The data supporting this article have been included as part of the ESI.†

Conflicts of interest

There are no conflicts to declare.

Acknowledgements

The authors would like to acknowledge funding support from the National Science Foundation (NSF CMMI 2239408).

References

1 A. Zarrouki, E. Espinosa, C. Boisson and V. Monteil, Free Radical Copolymerization of Ethylene with Vinyl Acetate under Mild Conditions, *Macromolecules*, 2017, **50**, 3516–3523.
2 I. O. Salyer and A. S. Kenyon, Structure and Property Relationships in Ethylene–Vinyl Acetate Copolymers, *J. Polym. Sci.*, 1971, **9**, 3083–3103.
3 R. M. Patel, Types and Basics of Polyethylene, in *Handbook of Industrial Polyethylene and Technology*, ed. M. A. Spalding and A. M. Chatterjee, 2017, pp. 105–138.
4 Ethylene Vinyl Acetate (EVA) – Market Share Analysis, **https://www.globenewswire.com/news-release/2024/03/13/2845792/28124/en/Ethylene-Vinyl-Acetate-EVA-Market-Share-Analysis-Industry-Trends-Statistics-Growth-Forecasts-2019-2029.html** (accessed 2024-05-15).
5 K. M. McLoughlin, A. J. Oskouei, M. K. Sing, A. Bandegi, S. Mitchell, J. Kennedy, T. G. Gray and I. Manas-Zloczower, Thermomechanical Properties of Cross-Linked EVA: A Holistic Approach, *ACS Appl. Polym. Mater.*, 2023, **5**, 1430–1439.
6 W. Liu, Z. Gong and Y. Chen, Design of Interface Dynamic Cross-Linked Hybrid Network with Highly Improved Mechanical, Recycling and Adhesive Performance, *Chem. Eng. J.*, 2023, **471**, 144598.
7 H. Guo, L. Yue, G. Rui and I. Manas-Zloczower, Recycling Poly(Ethylene-Vinyl Acetate) with Improved Properties through Dynamic Cross-Linking, *Macromolecules*, 2020, **53**, 458–464.
8 W. Guo, Z. Liu, S. Yang and L. Li, Fabrication of Sustainable Composite Foam from Ethylene Vinyl Acetate-Based Sole Waste via Solid-State Shear Milling and Supercritical Carbon Dioxide Foaming Technologies, *ACS Sustainable Chem. Eng.*, 2023, **11**, 13918–13927.
9 C. Z. Paiva Junior, R. S. Peruchi, F. d. C. Fim, W. d. O. S. Soares and L. B. da Silva, Performance of Ethylene Vinyl Acetate Waste (EVA-w) When Incorporated into Expanded EVA Foam for Footwear, *J. Cleaner Prod.*, 2021, **317**, 128352.
10 G. Sang, Y. Zhu and G. Yang, Mechanical Properties of High Porosity Cement-Based Foam Materials Modified by EVA, *Constr. Build. Mater.*, 2016, **112**, 648–653.
11 P. R. L. Lima, M. B. Leite and E. Q. R. Santiago, Recycled Lightweight Concrete Made from Footwear Industry Waste and CDW, *Waste Manage.*, 2010, **30**, 1107–1113.
12 N. Dulsang, P. Kasemsiri, P. Posi, S. Hiziroglu and P. Chindaprasirt, Characterization of an Environment Friendly Lightweight Concrete Containing Ethyl Vinyl Acetate Waste, *Mater. Des.*, 2016, **96**, 350–356.
13 T. J. Fazekas, J. W. Alty, E. K. Neidhart, A. S. Miller, F. A. Leibfarth and E. J. Alexanian, Diversification of Aliphatic C-H Bonds in Small Molecules and Polyolefins through Radical Chain Transfer, *Science*, 2022, **375**, 545–550.
14 S. Sharma and A. Bhattacharya, Drinking Water Contamination and Treatment Techniques, *Appl. Water Sci.*, 2016, **7**, 1043–1067.
15 P. Samanta, S. Let, W. Mandal, S. Dutta and S. K. Ghosh, Luminescent Metal–Organic Frameworks (LMOFs) as Potential Probes for the Recognition of Cationic Water Pollutants, *Inorg. Chem. Front.*, 2020, **7**, 1801–1821.
16 V. Beaugeard, J. Muller, A. Graillot, X. Ding, J. J. Robin and S. Monge, Acidic Polymeric Sorbents for the Removal of Metallic Pollution in Water: A Review, *React. Funct. Polym.*, 2020, **152**, 104599.
17 F. Dixit, R. Dutta, B. Barbeau, P. Berube and M. Mohseni, PFAS Removal by Ion Exchange Resins: A Review, *Chemosphere*, 2021, **272**, 129777.
18 A. M. James, S. Harding, T. Robshaw, N. Bramall, M. D. Ogden and R. Dawson, Selective Environmental Remediation of Strontium and Cesium Using Sulfonated Hyper-Cross-Linked Polymers (SHCPs), *ACS Appl. Mater. Interfaces*, 2019, **11**, 22464–22473.
19 H. Xu, B. Liu and M. Zhang, Preparation and application of monodisperse, highly cross-linked, and porous polystyrene microspheres for dye removal, *Colloids Surf., A*, 2022, **650**, 129596.
20 A. Martínez-García, A. S. Reche and J. M. Martín-Martínez, Improved Adhesion of EVAs with Different Vinyl Acetate Contents Treated with Sulphuric Acid, *J. Adhes. Sci. Technol.*, 2004, **18**, 967–982.
21 W. Marconi, R. Marcone and A. Piozzi, Sulfation and Preliminary Biological Evaluation of Ethylene-Vinyl Alcohol Copolymers, *Macromol. Chem. Phys.*, 2000, **201**, 715–721.
22 A. K. Phillips and R. B. Moore, Ionic Actuators Based on Novel Sulfonated Ethylene Vinyl Alcohol Copolymer Membranes, *Polymer*, 2005, **46**, 7788–7802.

Open Access Article. Published on 02 spalio 2024. Downloaded on 2025-08-07 08:12:29.
This article is licensed under a Creative Commons Attribution 3.0 Unported Licence.

23 Y. T. Sung, C. K. Kum, H. S. Lee, J. S. Kim, H. G. Yoon and W. N. Kim, Effects of Crystallinity and Crosslinking on the Thermal and Rheological Properties of Ethylene Vinyl Acetate Copolymer, *Polymer*, 2005, **46**, 11844–11848.
24 M. C. Costache, D. D. Jiang and C. A. Wilkie, Thermal Degradation of Ethylene–Vinyl Acetate Coplymer Nanocomposites, *Polymer*, 2005, **46**, 6947–6958.
25 A. R. Postema, H. De Groot and A. J. Pennings, Amorphous Carbon Fibres from Linear Low Density Polyethylene, *J. Mater. Sci.*, 1990, **25**, 4216–4222.
26 S. Horikiri, J. Iseki and M. Minobe, Process for production of carbon fiber. *U.S. Patent*, 4070446A, 1978.
27 A. G. Obando, M. Robertson, C. Umeojiakor, P. Smith, A. Griffin, Y. Xiang and Z. Qiang, Catalyst-Free Upcycling of Crosslinked Polyethylene Foams for CO2 Capture, *J. Mater. Res.*, 2024, **39**, 115–125.
28 G. Lee, M. E. Lee, S. S. Kim, H. I. Joh and S. Lee, Efficient Upcycling of Polypropylene-Based Waste Disposable Masks into Hard Carbons for Anodes in Sodium Ion Batteries, *J. Ind. Eng. Chem.*, 2022, **105**, 268–277.
29 M. Robertson, A. Griffin, A. G. Obando, A. Barbour, R. Davis and Z. Qiang, Precursor Design for Efficient Synthesis of Large-Pore, Sulfur-Doped Ordered Mesoporous Carbon through Direct Pyrolysis, *Mol. Syst. Des. Eng.*, 2023, **8**, 1156–1164.
30 M. Robertson, A. Barbour, A. Griffin, A. G. Obando, P. Smith and Z. Qiang, Sulfonation-Induced Cross-Linking and Nanostructural Evolution of a Thermoplastic Elastomer for Ordered Mesoporous Carbon Synthesis: A Mechanistic Study, *ACS Appl. Eng. Mater.*, 2023, **1**, 2577–2588.
31 Y. Zhang, L. Tan, A. Yao, P. Tan, R. Guo, M. Zhou, P. Zhu, S. Huang and Y. Wu, Improvement of Filtration Performance of Polyvinyl Chloride/Cellulose Acetate Blend Membrane via Acid Hydrolysis, *J. Appl. Polym. Sci.*, 2021, **138**, 50312.
32 M. Robertson, A. Guillen-Obando, A. Barbour, P. Smith, A. Griffin and Z. Qiang, Direct Synthesis of Ordered Mesoporous Materials from Thermoplastic Elastomers, *Nat. Commun.*, 2023, **14**, 639.
33 P. Smith, A. G. Obando, A. Griffin, M. Robertson, E. Bounds and Z. Qiang, Additive Manufacturing of Carbon Using Commodity Polypropylene, *Adv. Mater.*, 2023, 2208029.
34 J. Wolska, M. Muńko, H. El Siblani, I. Telegeiev, M. Frankowski, A. Szwajca, J. Walkowiak-Kulikowska, M. El-Roz and L. Wolski, The Influence of Cross-Linking Density on the Efficiency of Post-Synthetic Sulfonation of Hyper-Cross-Linked Polymers and Their Adsorption Capacity for Antibiotic Pollutants, *J. Environ. Chem. Eng.*, 2023, **11**, 110429.
35 J. Wolska, M. Frankowski, J. Jenczyk and L. Wolski, Highly Sulfonated Hyper-Cross-Linked Polymers as Promising Adsorbents for Efficient and Selective Removal of Ciprofloxacin from Water, *Sep. Purif. Technol.*, 2024, **343**, 127147.
36 A. Blocher, F. Mayer, P. Schweng, T. M. Tikovits, N. Yousefi and R. T. Woodward, One-Pot Route to Fine-Tuned Hypercrosslinked Polymer Solid Acid Catalysts, *Mater. Adv.*, 2022, **3**, 6335.
37 G. Xiong, Q. Zhang, B. Ren, L. You, F. Ding, Y. He, X. Fan, N. Wang and Y. Sun, Highly Efficient and Selective Adsorption of Cationic Dyes in Aqueous Media on Microporous Hyper Crosslinked Polymer with Abundant and Evenly Dispersed Sulfonic Groups, *ChemistrySelect*, 2020, **5**, 6541–6548.
38 C. K. Shaha, M. A. A. Mahmud, S. Saha, S. Karmaker and T. K. Saha, Efficient Removal of Sparfloxacin Antibiotic from Water Using Sulfonated Graphene Oxide: Kinetics, Thermodynamics, and Environmental Implications, *Sep. Purif. Technol.*, 2024, **343**, 1383–5866.
39 S. Mani and R. N. Bharagava, Exposure to Crystal Violet, Its Toxic, Genotoxic and Carcinogenic Effects on Environment and Its Degradation and Detoxification for Environmental Safety, *Rev. Environ. Contam. Toxicol.*, 2016, **237**, 71–104.
40 P. O. Oladoye, T. O. Ajiboye, E. O. Omotola and O. J. Oyewola, Methylene Blue Dye: Toxicity and Potential Elimination Technology from Wastewater, *Results Eng.*, 2022, **16**, 100678.
41 W. Tan, X. Xu, Y. Lv, W. Lei, K. Hu, F. Ye and S. Zhao, Sulfonic Acid Functionalized Hierarchical Porous Covalent Organic Frameworks as a SALDI-TOF MS Matrix for Effective Extraction and Detection of Paraquat and Diquat, *J. Colloid Interface Sci.*, 2021, **603**, 172–181.
42 Y. Li, S. Wang, Z. Shen, X. Li, Q. Zhou, Y. Sun, T. Wang, Y. Liu and Q. Gao, Gradient Adsorption of Methylene Blue and Crystal Violet onto Compound Microporous Silica from Aqueous Medium, *ACS Omega*, 2020, **5**, 28382–28392.
43 M. I. Khan, T. K. Min, K. Azizli, S. Sufian, H. Ullah and Z. Man, Effective Removal of Methylene Blue from Water Using Phosphoric Acid Based Geopolymers: Synthesis, Characterizations and Adsorption Studies, *RSC Adv.*, 2015, **5**, 61410–61420.
44 M. Maruthapandi, V. B. Kumar, J. H. T. Luong and A. Gedanken, Kinetics, Isotherm, and Thermodynamic Studies of Methylene Blue Adsorption on Polyaniline and Polypyrrole Macro-Nanoparticles Synthesized by C-Dot-Initiated Polymerization, *ACS Omega*, 2018, **3**, 7196–7203.
45 C. Zhou, Q. Wu, T. Lei and I. I. Negulescu, Adsorption Kinetic and Equilibrium Studies for Methylene Blue Dye by Partially Hydrolyzed Polyacrylamide/Cellulose Nanocrystal Nanocomposite Hydrogels, *Chem. Eng. J.*, 2014, **251**, 17–24.
46 S. Pal, S. Ghorai, C. Das, S. Samrat, A. Ghosh and A. B. Panda, Carboxymethyl Tamarind-g-Poly(Acrylamide)/Silica: A High Performance Hybrid Nanocomposite for Adsorption of Methylene Blue Dye, *Ind. Eng. Chem. Res.*, 2012, **51**, 15546–15556.
47 A. Aluigi, F. Rombaldoni, C. Tonetti and L. Jannoke, Study of Methylene Blue Adsorption on Keratin Nanofibrous Membranes, *J. Hazard. Mater.*, 2014, **268**, 156–165.
48 X. Liu, Y. Zhang, H. Ju, F. Yang, X. Luo and L. Zhang, Uptake of Methylene Blue on Divinylbenzene Cross-Linked

 © 2024 The Author(s). Published by the Royal Society of Chemistry

Open Access Article. Published on 02 spalio 2024. Downloaded on 2025-08-07 08:12:29.
This article is licensed under a Creative Commons Attribution 3.0 Unported Licence.

Chitosan/Maleic Anhydride Polymer by Adsorption Process, *Colloids Surf., A*, 2021, **629**, 127424.

49 Y. Yang, Y. Xie, L. Pang, M. Li, X. Song, J. Wen and H. Zhao, Preparation of Reduced Graphene Oxide/Poly (Acrylamide) Nanocomposite and Its Adsorption of Pb(II) and Methylene Blue, *Langmuir*, 2013, **29**, 10727–10736.

50 S. Thakur, S. Pandey and O. A. Arotiba, Development of a Sodium Alginate-Based Organic/Inorganic Superabsorbent Composite Hydrogel for Adsorption of Methylene Blue, *Carbohydr. Polym.*, 2016, **153**, 34–46.

51 J. Fu, Z. Chen, M. Wang, S. Liu, J. Zhang, J. Zhang, R. Han and Q. Xu, Adsorption of Methylene Blue by a High-Efficiency Adsorbent (Polydopamine Microspheres): Kinetics, Isotherm, Thermodynamics and Mechanism Analysis, *Chem. Eng. J.*, 2015, **259**, 53–61.

52 Z. Chen, J. Zhang, J. Fu, M. Wang, X. Wang, R. Han and Q. Xu, Adsorption of Methylene Blue onto Poly (Cyclotriphosphazene-Co-4,4′-Sulfonyldiphenol) Nanotubes: Kinetics, Isotherm and Thermodynamics Analysis, *J. Hazard. Mater.*, 2014, **273**, 263–271.

53 Z. Chen, J. Fu, M. Wang, X. Wang, J. Zhang and Q. Xu, Adsorption of Cationic Dye (Methylene Blue) from Aqueous Solution Using Poly(Cyclotriphosphazene-Co-4,4′-Sulfonyldiphenol) Nanospheres, *Appl. Surf. Sci.*, 2014, **289**, 495–501.

54 H. Su, W. Li, Y. Han and N. Liu, Magnetic Carboxyl Functional Nanoporous Polymer: Synthesis, Characterization and Its Application for Methylene Blue Adsorption, *Sci. Rep.*, 2018, **8**, 6506.

55 D. Gan, J. Dou, Q. Huang, H. Huang, J. Chen, M. Liu, H. Qi, Z. Yang, X. Zhang and Y. Wei, Carbon Nanotubes-Based Polymer Nanocomposites: Bio-Mimic Preparation and Methylene Blue Adsorption, *J. Environ. Chem. Eng.*, 2020, **8**, 103525.

56 M. M. Ayad and A. A. El-Nasr, Adsorption of Cationic Dye (Methylene Blue) from Water Using Polyaniline Nanotubes Base, *J. Phys. Chem. C*, 2010, **114**, 14377–14383.

57 N. Dahdouh, S. Amokrane, R. Murillo, E. Mekatel and D. Nibou, Removal of Methylene Blue and Basic Yellow 28 Dyes from Aqueous Solutions Using Sulphonated Waste Poly Methyl Methacrylate, *J. Polym. Environ.*, 2020, **28**, 271–283.

58 S. Sabar, H. Abdul Aziz, N. H. Yusof, S. Subramaniam, K. Y. Foo, L. D. Wilson and H. K Lee, Preparation of Sulfonated Chitosan for Enhanced Adsorption of Methylene Blue from Aqueous Solution, *React. Funct. Polym.*, 2020, **151**, 104584.

59 N. Chailek, D. Daranarong, W. Punyodom, R. Molloy and P. Worajittiphon, Crosslinking Assisted Fabrication of Ultrafine Poly(Vinyl Alcohol)/Functionalized Graphene Electrospun Nanofibers for Crystal Violet Adsorption, *J. Appl. Polym. Sci.*, 2018, **135**, 46318.

60 S. R. Shirsath, A. P. Patil, B. A. Bhanvase and S. H. Sonawane, Ultrasonically Prepared Poly(Acrylamide)-Kaolin Composite Hydrogel for Removal of Crystal Violet Dye from Wastewater, *J. Environ. Chem. Eng.*, 2015, **3**, 1152–1162.

61 S. Li, Removal of Crystal Violet from Aqueous Solution by Sorption into Semi-Interpenetrated Networks Hydrogels Constituted of Poly(Acrylic Acid-Acrylamide-Methacrylate) and Amylose, *Bioresour. Technol.*, 2010, **101**, 2197–2202.

62 S. Chakraborty, S. Chowdhury and P. D. Saha, Adsorption of Crystal Violet from Aqueous Solution onto NaOH-Modified Rice Husk, *Carbohydr. Polym.*, 2011, **86**, 1533–1541.

63 J. Qin, F. Qiu, X. Rong, J. Yan, H. Zhao and D. Yang, Adsorption Behavior of Crystal Violet from Aqueous Solutions with Chitosan–Graphite Oxide Modified Polyurethane as an Adsorbent, *J. Appl. Polym. Sci.*, 2015, **132**, 41828.

64 G. Sharma, A. Kumar, M. Naushad, A. García-Peñas, A. H. Al-Muhtaseb, A. A. Ghfar, V. Sharma, T. Ahamad and F. J. Stadler, Fabrication and Characterization of Gum Arabic-Cl-Poly(Acrylamide) Nanohydrogel for Effective Adsorption of Crystal Violet Dye, *Carbohydr. Polym.*, 2018, **202**, 444–453.

65 M. Gholami, M. T. Vardini and G. R. Mahdavinia, Investigation of the Effect of Magnetic Particles on the Crystal Violet Adsorption onto a Novel Nanocomposite Based on κ-Carrageenan-g-Poly(Methacrylic Acid), *Carbohydr. Polym.*, 2016, **136**, 772–781.

66 M. M. A. Hameed, F. A. Al-Aizari and B. M. Thamer, Synthesis of a Novel Clay/Polyacrylic Acid-Tannic Acid Hydrogel Composite for Efficient Removal of Crystal Violet Dye with Low Swelling and High Adsorption Performance, *Colloids Surf., A*, 2024, **684**, 133130.

67 A. Saeed, M. Sharif and M. Iqbal, Application Potential of Grapefruit Peel as Dye Sorbent: Kinetics, Equilibrium and Mechanism of Crystal Violet Adsorption, *J. Hazard. Mater.*, 2010, **179**, 564–572.

68 A. Essekri, M. A. Haki, M. Laabd, A. A. Addi, R. Lakhmiri and A. Albourine, Citric Acid-Functionalized Acacia Pods as a Robust Biosorbent for Decontamination of Wastewater Containing Crystal Violet Dye: Experimental Study Combined with Statistical Optimization, *Chem. Eng. Res. Des.*, 2023, **195**, 390–403.

69 M. Loganathan, A. S. Raj, A. Murugesan and P. S. Kumar, Effective Adsorption of Crystal Violet onto Aromatic Polyimides: Kinetics and Isotherm Studies, *Chemosphere*, 2022, **304**, 135332.

70 M. Massoudinejad, H. Rasoulzadeh and M. Ghaderpoori, Magnetic Chitosan Nanocomposite: Fabrication, Properties, and Optimization for Adsorptive Removal of Crystal Violet from Aqueous Solutions, *Carbohydr. Polym.*, 2019, **206**, 844–853.